DESIGN AND EXPERIMENT OF AN AUTOMATIC GIRDLING DEVICE FOR ECONOMIC TREE TRUNK INSPIRED BY CAM MECHANISM
/
凸轮原理启发的经济林树干自动环剥装置的设计与实验研究

Zhenkun ZHI[1], Haifeng LUO[*]
[1]School of Engineering, Beijing Forestry University, Beijing/ China;
Tel: 8601062338144; E-mail: luohaifeng@bjfu.edu.cn
DOI: https://doi.org/10.35633/inmateh-72-04

Keywords: *cam mechanism, half-ring, tree trunk profile scanning, trajectory calculating, chainsaws*

ABSTRACT
In order to solve the problem of complicated processes, low efficiency and high cost of economic tree trunks girdling, inspired by cam mechanism this study developed a new type of automatic half-ring girdling device, which can automatically complete a series of operations, including the tree trunk profile scanning, girdling trajectory calculating and automatic bark cutting. A pair of laser rangefinders and guide screws were symmetrically arranged on a half-ring rotating rail, which could rotate around the tree trunk, and two chainsaws assembled above the guide screws were controlled to move radially. The laptop was used as upper computer, and a 4-axis motion control card was used as the lower computer, which constituted the control system of precise movement. The programs of the tree trunk profile scanning, the xylem profile curve fitting and the chainsaw centre trajectory calculation were designed in LabVIEW. The scanning tests and girdling experiments were carried out on the different sections of the tree trunks in the laboratory. The feasibility of the automatic girdling device for economic tree trunks was verified with one complete and automatic girdling operation finished by this device, which took 150 seconds, and the error range of automatic girdling was within ±2mm. This device improves the automation degree of girdling operation and provides a support for the development of economic forestry.

摘要
为解决经济林树木开甲存在流程复杂，效率低，成本高的问题，受凸轮原理启发，本文设计一种新型自动化半环开甲装置，自动完成树干轮廓扫描，环剥轨迹计算，自动切割树皮等操作。该装置在半环转动支架上对称安装了一对称双激光测距仪、丝杠，半环支架可环绕树干旋转运动。丝杠上面安装的手持电锯能够实现径向运动。以 LabVIEW 为上位机，以 4 轴运动控制卡作为下位机，构成精确运动的控制系统。在 LabVIEW 中完成了树干轮廓扫描、木质部轮廓曲线拟合、电锯中心轨迹计算等程序设计。在实验室中对树干不同的截面进行了测量实验和环剥实验。完整自动的开甲操作证实了该经济林开甲装置的可行性，该装置单次自动环剥时间为 150 秒，开甲精度为±2mm。该装置提高了开甲操作的自动化程度，为经济林产业提供了支撑。

INTRODUCTION
Girdling is defined as the removal of a ring of bark or phloem, mainly around the trunk or branch, which has the immediate effect of blocking the phloem transport pathway, thereby eliciting the accumulation of carbohydrates above the girdle *(Goren et al., 2004; Oberhunber et al., 2017)*. In 1686, Marcello Malpighi carried out the classical experiment of organic solute migration with removal of the bark around the trunk of a tree in a circular pattern. Since Kobel studied the physiological mechanism of flower promotion by ring cutting from the perspective of C/N ratio in 1931, many scholars had carried out in-depth studies from different perspectives such as nutrition, hormone and nucleic acid. Particularly, girdling often promotes flower-bud initiation, fruit set and growth, and increases yield, but reduces vegetative growth. Thus, girdling is widely applied for hundreds of years in trees horticultural practice because of these benefits *(Wilkie et al., 2008; De Schepper and Steppe, 2011)*. The jujube tree is an important economic crop native to China, which accounts for more than 98% of the total cultivated area in the world. Girdling jujube trees at the right stage of growth can effectively increase the fruit set rate of jujube trees, improve fruit quality, and increase production at the same time (*Ye et al., 2019*). Therefore, girdling is often used to regulate the growth of fruit trees and promote fruit development.

Girdling improves the fruit-set rate of citrus *(Yang et al., 2013)*, persimmon *(Juan et al., 2009)*, grape *(Zhu et al., 2022)*, tomato *(Chai et al., 2021)*, and finally increases the fruit yield. Therefore, girdling technology is widely used in economic forestry.

The using of different tools directly affects the girdling efficiency of fruit trees, ultimately the yield of economic trees. Traditionally, girdling is accomplished by workers using simple hand-held knives to remove the tree bark. The typical girdling tools are "Z" type girdling knife, triangular double-edged ring cutter knife, curved bar double-edged ring cutter, L-shaped ring stripper, pulley girdling knife, double curved blade ring stripping shears, three-blade ring stripper *(Duan, 2007)*. The structures of these girdling tools are simple and the effects of girdling depend largely on the experience of workers. Girdling work is labour-intensive and time-consuming, and this problem becomes serious when huge amount of fruit trees needs to be girdled within a short period, especially with the yearly reduction of the workforce. In response to the problems of low quality and efficiency of general artificial girdling tools, an electric type jujube girdling device was designed *(Xie, et al., 2018)*. This type of girdling device solved the problem of maintaining relative fixation with the trunk during girdling, but it led to another problem of uncontrollable girdling breakage rate by fixing the tool to perform girdling at the same depth. *Li, et al., (2019)*, designed a handheld small girdling device, which improved the efficiency of cutting bark, but the accuracy of girdling was also dependent on workers' experience. Although the electric girdling tools increased the speed of working, accuracy and efficiency of traditional girdling still varied from person to person.

In this paper, a new automatic girdling device is designed to improve girdling accuracy on the basis of ensuring efficiency of girdling. A half-ring symmetrical mechanical structure is adopted on the device, and actuators and scanning sensors are selected based on the requirements of economic trees girdling. The control flow is completed according to the structure of the girdling device and the girdling process, and girdling programs are designed in LabVIEW. Three levels of error analysis are carried out by scanning tests and girdling experiments in laboratory.

MATERIALS AND METHODS

The economic trees that need to increase production, should be girdled when they are older than 7 years or the trunk diameters are greater than 10 cm. Nearly half of the time of flowering is the best time to be girdled. One of the manual girdling methods is shown in Fig. 1. The operators select a position 30 cm above the ground, and the old bark is removed from the tree trunk by a sickle. The width of the excised skin should be widened to 2 cm, and the inner phloem exposes a circle with a width of 1 cm. The upper part of the phloem needs to be cut by tools after peeling horizontally to the xylem of the tree, and it is cross cut obliquely at the lower part of the phloem to the xylem. The final incision width should be controlled at about 0.5 cm. Due to the different sizes of tree trunks and the experience of workers, the time for manual girdling usually varies from minutes to half an hour. In some regions of China, experienced workers girdle about 200 trees for 400-500 yuan (RMB) a day.

Fig. 1 – Manual girdling

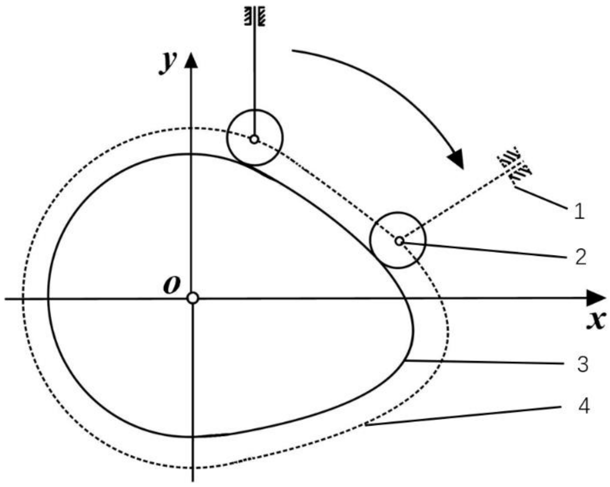

Fig. 2 – The inversion of cam
1–Guide; 2–Roller; 3–Cam; 4–The trajectory of roller centre;

Core mechanisms

As shown in Fig. 2, an irregularly shaped cam (3) is fixed at point O. The roller (2) can be rotated relative to the cam together with the guide, and also be moved radially inside the guide (1). The trajectory (4) of the roller can be formed by synthetic motion of radial slide and rotation. In this paper, the xylem of the tree trunk is taken as the cam, and the chainsaw for girdling is considered as the roller. Based on the principle of inversion of cam mechanism shown in Fig. 2, the trajectory (4) of the chainsaw's centre can be obtained for the automatic girdling method.

The core working principle of the device is shown in Fig. 3. A pair of chainsaws (3), guide screws (2) and laser rangefinders (1) are mounted symmetrically at the end of the half-ring rail (6). As shown in Fig. 3a, the profile of the tree trunk is scanned by the device. The scanning starts at the horizontal initial position (7). The half-ring rail rotates counter clockwise around the tree trunk, and at the same time the laser rangefinders start measuring along the red dashed circle. The distance between the laser rangefinders and the tree trunk is measured by the laser rangefinders at a certain frequency in the process of rotational movement. The half-ring rail reaches the opposite horizontal position (8) after the scanning of the tree trunk profile. The external profile of the tree trunk (5) is obtained, and the xylem profile curve (4) is acquired by algorithms. The girdling process of the device is shown in Fig. 3b. The half-ring rail rotates clockwise, and the chainsaws are driven to girdle based on trajectory mentioned in Fig. 2. The device completes girdling when the half-ring rail rotates to the initial position (7) in Fig. 3a.

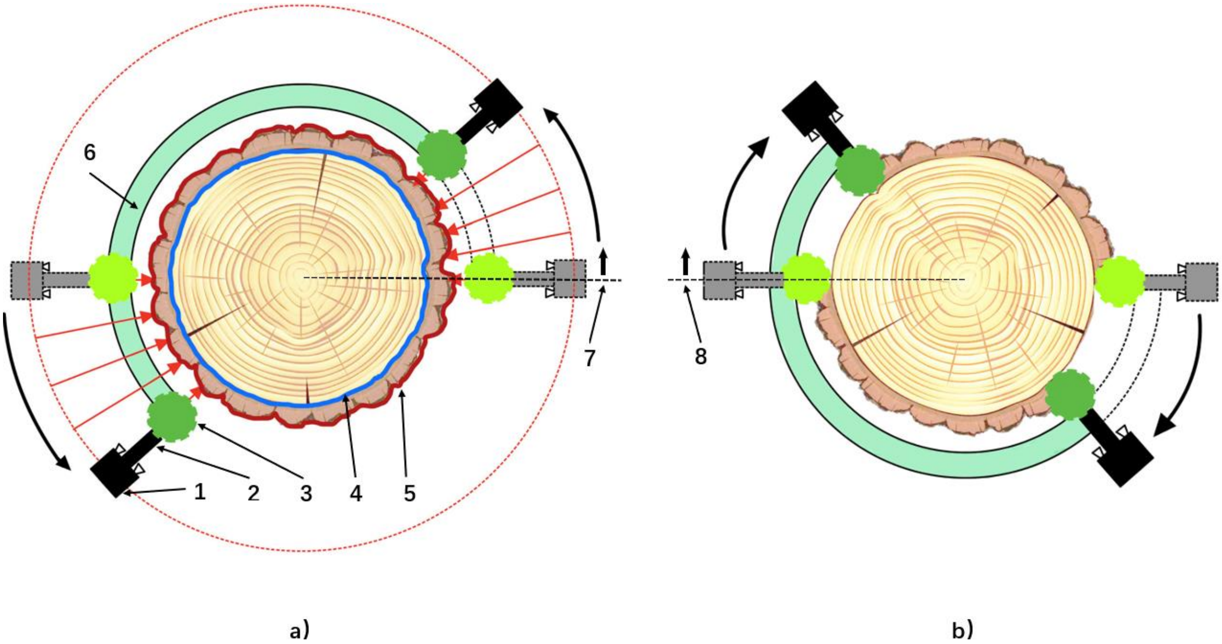

Fig. 3 – The girdling device mechanism

a) The scanning process; b) The girdling process

1-Laser rangefinders; 2-Guide screws; 3-Chainsaws; 4-Xylem profile curve; 5-Tree trunk profile curve; 6-Half-ring rail; 7-Initial position of scanning; 8-Initial position of girdling

As shown in Fig. 4, the motion centre O of the half-ring rail is taken as the origin of the cartesian coordinate system, and curve C is the trajectory of the half-ring rail. The xylem profile curve s is obtained by calculating based on the tree trunk profile, and its polar coordinate equation is $s=s(\varphi)$. The instantaneous girdling state of the chainsaw with B as the centre at the cutting point A is shown in Fig. 4. The polar coordinate of point A is $(\varphi, s(\varphi))$. The tangent line of A point on the curve s is l'. The common normal line through A point is l, and the angle between l and the positive direction of x axis is β, then the cartesian coordinate of A point is:

$$\begin{aligned} x &= s\cos\varphi \\ y &= s\sin\varphi \end{aligned} \tag{1}$$

Line l and l' are perpendicular to each other, the trigonometric function of the angle β is:

$$\tan\beta = -\frac{dx}{dy} \tag{2}$$

$$\sin\beta = \frac{dx/d\varphi}{\sqrt{(dx/d\varphi)^2 + (dy/d\varphi)^2}} \tag{3}$$

$$\cos\beta = \frac{-dy/d\varphi}{\sqrt{(dx/d\varphi)^2 + (dy/d\varphi)^2}} \tag{4}$$

The radius of the chainsaw is R, and the coordinate of $B(X,Y)$ on the central trajectory of the chainsaw is obtained as follows :

$$\begin{aligned} X &= x + R\cos\beta \\ Y &= y + R\sin\beta \end{aligned} \tag{5}$$

In order to be used directly in control program, the cartesian coordinate on trajectory B is transformed into a polar coordinate relative to point O as follows.

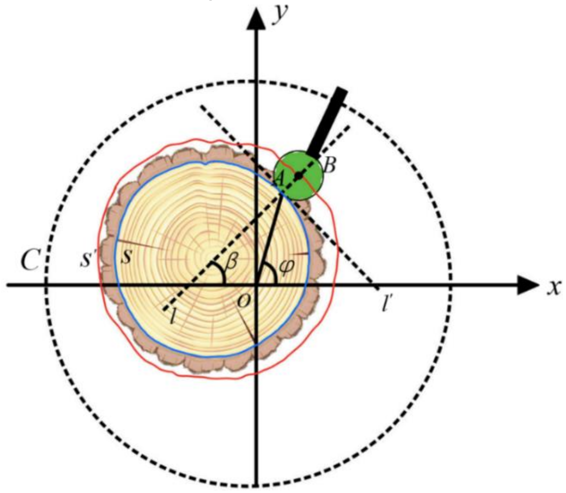

Fig. 4 – The principle of the trajectory of the chainsaw's centre

Overall structure

The mechanical structure of the device is shown in Fig. 5. The half-ring rail (5) is driven by stepper motor (1) to rotate around the tree trunk (6) though gearing. Two laser rangefinders (2) are symmetrically installed at both ends of the half-ring rail, which realizes the scanning of the tree trunk in rotational movement. The guide screws and chainsaws are mounted at the end of the half-ring rail by the way the same to laser rangefinders. The guide screws are driven by motors to realize the radial movement. Girdling can be completed by the chainsaws with synthetic movement of radial movement and rotational movement.

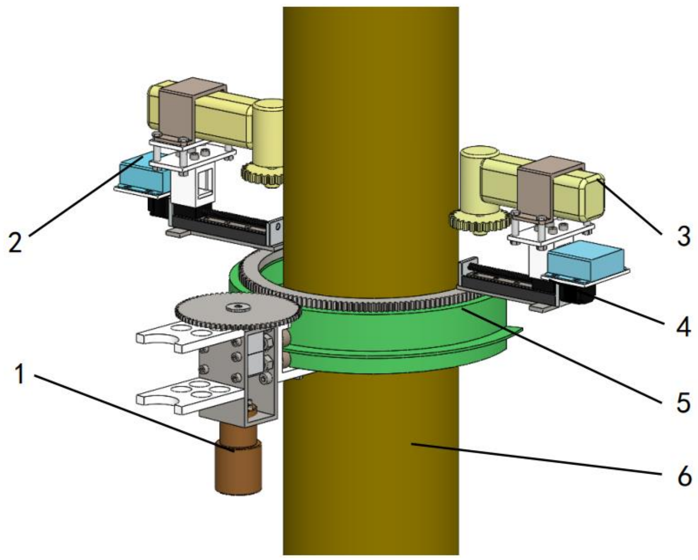

Fig. 5 – The girdling device

1-Stepper motor; 2-Laser rangefinders; 3-Chainsaws; 4-Guide screw motors; 5-Half-ring rail; 6-Tree trunk

Control system

The overall hardware system of the girdling device is shown in Fig. 6. The laptop based on x64 Intel (R) i7 processor is selected as the upper computer of the device control system. *Art* 1020 motion control card is selected as the lower computer. *Art* 1020 is a four-axis servo/stepper motor motion control card with the USB bus, which can complete various complex control requirements of servo / stepper motor. The motors in this girdling device are controlled by *Art* 1020 precisely. Guide screw motors and stepper motor are used as the drive system, and the laser rangefinders are the sensors of the scanning system. The transmission of scanning signals and control signals between laptop and laser rangefinders is realized through USB bus. The hardware parameters are shown in Table 1.

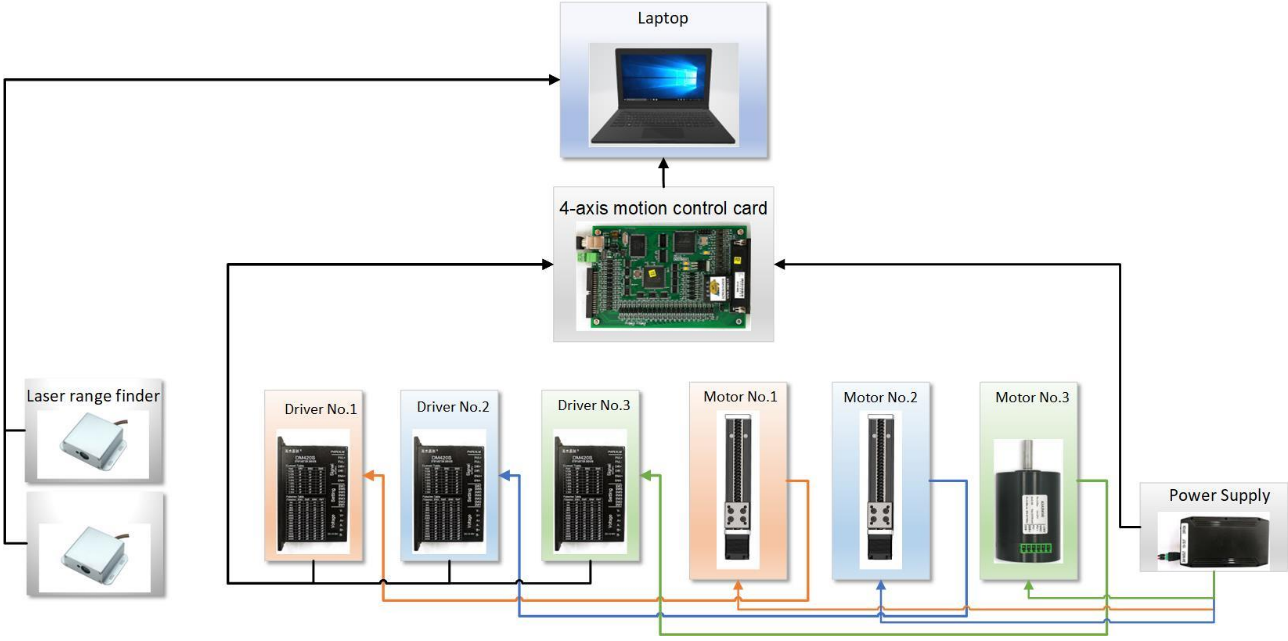

Fig. 6 – Hardware system of girdling device

Table 1

Main technical parameters

Parameter	Value	Units
Scanning Frequency	1~20	Hz
Stepper motor torque	20	N·m
Stepper motor power	50	W
Accuracy of guide screw	0.125	mm
Motor response frequency	≤80k	Hz
Laser rangefinder measurement accuracy	±0.05	mm

The block diagram of the control system program is shown in Fig. 7. In order to ensure the accuracy of the movement, the initialization of the girdling device control system is first carried out. The parameters including the emission frequency of laser rangefinders, scanning time and cutting time are set after initialization. Then the half-ring rail is driven by the stepper motor to rotate around the tree trunk. simultaneously, the laser rangefinders are started to scan the tree trunk. The half-ring rail rotates to the position (8) as mentioned in Fig. 3b after finishing scanning. The polar coordinate points of the tree trunk external profile are saved in a txt file. The data processing includes two algorithms. Since an explicit function between the bark profile and its xylem profile has not been defined in the papers, this paper proposes the interval minimum algorithm. Analysis of the bark and xylem structure through the trunk cross-section shows that the change in curvature of the xylem profile surface is much smaller than that of the bark profile surface. The measured polar coordinate points saved in the txt file are grouped into equal intervals according to the scanning direction. The first smallest value in the interval is selected as the representative point close to the xylem. The interval minimum curve is obtained by linear fitting of these selected points. Then the xylem profile curve, which is also the curve s mentioned in Fig. 4, is obtained according to the thickness value of the tree bark. The trajectory of the chainsaw centre is obtained by the cam inversion algorithm based on the equation (5). The cutting operation starts at the position (8) in Fig. 3b.

The laptop converts the polar coordinate points of chainsaw centre trajectory into pulse signals to 4-aix motion control card. The stepper motor and the guide screw motors are controlled according to the pulse signals, and the girdling is carried out with the half-ring rail moving clockwise. The girdling operation of the tree trunk is completed by chainsaws with radial and rotational synthetic movement.

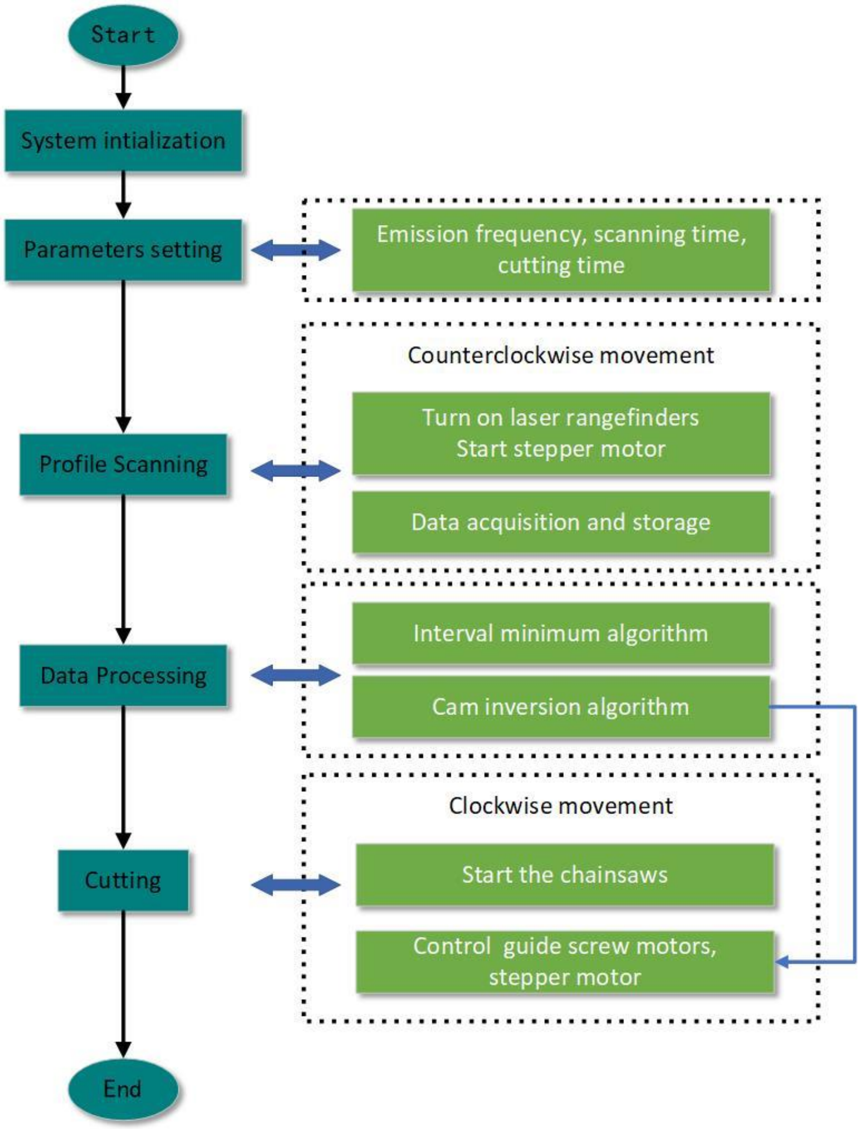

Fig. 7 – Control system program block diagram

As shown in Fig.8, the operation panel of the girdling device control system is designed in LabVIEW. The operation panel includes the parameters setting, the status prompt of the completed process, the real-time display of scanning state and cutting state, and the schematic display of current girdling state. The scanning time, scanning frequency and cutting time can be set on the panel based on different girdling requirements of economic tree trunks. The process of girdling can be divided into four parts according to control system program block diagram, and every part can be controlled individually by the button in the panel. Every finished part can be prompted by the indicator light behind the corresponding button. In the part of real-time scanning, the scanning and cutting process of the tree trunk profile can be shown in the polar coordinate system in real time.

As shown in the polar coordinate system, the red curve is the profile of the tree trunk, and the brown curve is the profile of the xylem calculated by algorithm. The corresponding state in the part of real-time scanning is shown in form of pictures in the part of process. According to the real-time feedback in the panel, the operator can control the operation condition of the girdling device.

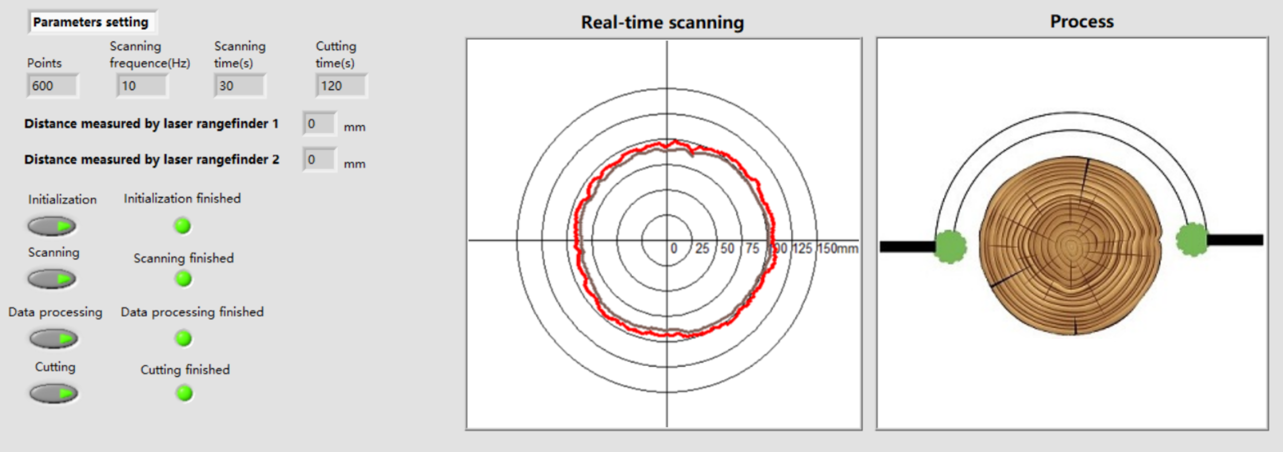

Fig. 8 – The operation panel of the control system

RESULTS AND DISCUSSION

Scanning system error

In the whole process of girdling, the scanning of the external profile of the tree trunk was completed first, and the scanning result was directly related to the accuracy of the centre point trajectory of the chainsaws obtained from the cam inversion algorithm. Therefore, the error analysis of the scanning system of the girdling device is carried out first. RA7525SE-1005 is a six-axis absolute arm, which can realize high-precision contact measurement. The measurement radius range of RA7525SE-1005 is 1.2 meters, and the measurement point repeatability accuracy is 0.050 mm. It can accurately measure the 3D coordinates of spatial points in its radius range. The cross sections of the same tree trunk were measured by the device and the RA7525SE-1005 respectively. In this experiment, a wooden pile only with its xylem was selected to be scanned. The profile scanning with the girdling device was shown in Fig.9, and the profile measurement with RA7525SE-1005 was shown in Fig.10.

Fig. 9 – Profile scanning with the girdling device

1-Girdling mechanical structure; 2-Control box; 3-Power; 4-Laptop;

Fig. 10 – Profile measurement with RA7525SE-1005

The same positions of the wooden pile were measured by RA7525SE-1005 and the girdling device. In the ten groups of scanning experiments, the scanning frequency of the laser rangefinders was 10 Hz, and the scanning time was from 7.5 s to 30 s.

The number of scanning points by the girdling device was from 150 to 600, and number of points measured by RA7525SE-1005 was 50. In order to better calculate the result error between the result measured by RA7525SE-1005 and the result scanned by girdling device, the measurement result of RA7525SE-1005 was fitted by first order. The measurement results were shown in Fig. 11.

Data 1 is the measurement result of RA7525SE-1005, and data 2 to data 11 were scanning results by the girdling device. Due to the high measurement precision of RA7525SE-1005, data 1 mentioned in Fig. 11 was taken as the standard value. In the polar coordinate system, the difference between points (data 2 to data 11) scanned by the girdling device and the fitted curve (data 1) at the corresponding angle was used as the error of the measurement system.

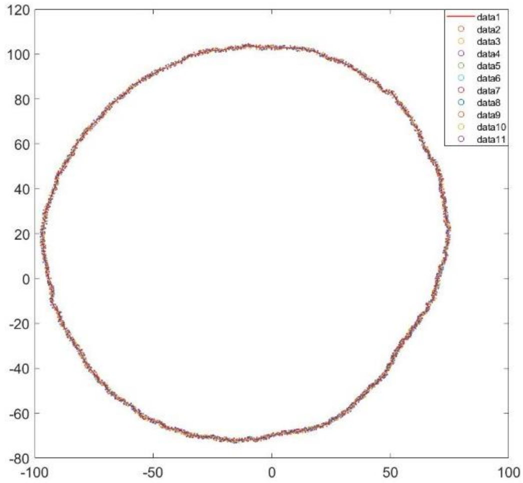

Fig. 11 – The measurement results

The error calculation results were shown in Table 2, including the measurement error maximum, measurement error minimum, measurement error average and root mean square error of measurement system. It can be concluded that the tree trunk profile scanning average error of the device was within 1 mm. With the increase of the number of measurement points, the error decreased in all four aspects. When the number of points measured reached 600, the average error stabilized within 0.5 mm and the root mean square error remained at a low level.

Table 2

Error of scanning system

Number of scanning points by girdling device	Number of measurement points by RA7525SE-1005	Maximum error (mm)	Minimum error(mm)	Average error(mm)	Root mean square error
150	50	1.994	-2.030	0.783	1.0293
200	50	1.984	-1.999	0.690	0.9909
250	50	1.979	-1.999	0.681	0.9350
300	50	1.977	-1.998	0.572	0.8133
350	50	1.953	-1.998	0.536	0.7872
400	50	1.918	-1.997	0.521	0.7805
450	50	1.853	-1.997	0.501	0.7486
500	50	1.758	-1.982	0.443	0.6610
550	50	1.740	-1.458	0.408	0.6316
600	50	1.668	-1.329	0.408	0.2828

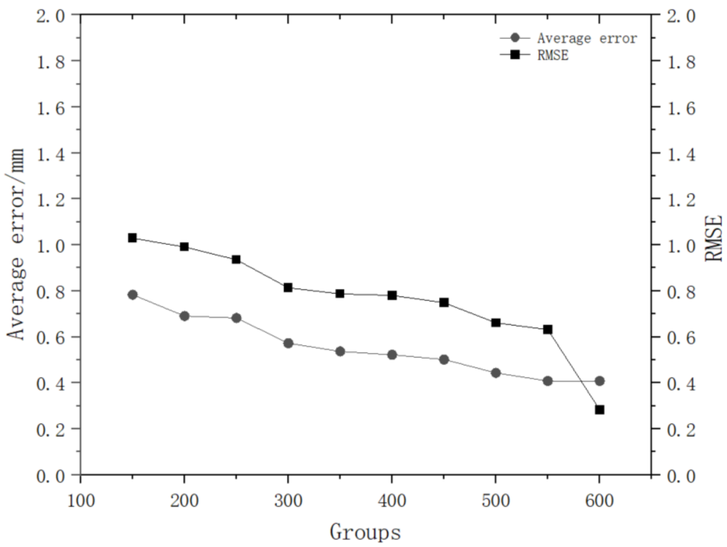

Fig. 12 – Error of scanning system

Control system and algorithm error

In this experiment, a wooden pile only with its xylem was selected to be cut. In the process of cutting, the error includes the scanning error, the motion control error and the calculation error of the cam inversion algorithm mentioned in Fig. 7. In order to reduce the impact of scanning error, 600 points were selected in the process of profile scanning. In this experiment, the wooden file was scanned in 30 seconds, and the chainsaw centre trajectory calculated by the cam inversion algorithm was performed in 120 seconds.

The process of scanning and cutting were shown in Fig. 13 and Fig. 14. In Fig. 15, the red curve was the profile of the wooden pile, and it was used as the curve s in Fig. 4, and the brown curve was the cutting profile. In this experiment, the cutting depth was 5 mm. The cutting depth errors were measured by 50 index vernier scale. There were ten groups of girdling experiments were carried out, and the number of error measurement points was 100 in each group.

Fig. 13 – Scanning

Fig. 14 – Cutting

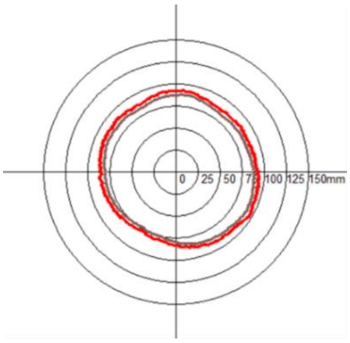

Fig. 15 – Scanning profile and cutting profile

Table 3

Error of control system and algorithm

Experimental group	Number of measurement points	Maximum error (mm)	Minimum error (mm)	Average error (mm)	Root mean square error
1	100	1.68	-1.56	0.74	0.8704
2	100	1.84	-1.48	0.68	0.8304
3	100	1.88	-1.78	0.64	0.7631
4	100	1.68	-1.78	0.74	0.9013
5	100	1.56	-1.86	0.58	0.7055
6	100	1.54	-1.84	0.76	0.9231
7	100	1.20	-1.78	0.70	0.8166
8	100	1.86	-1.84	0.78	0.9222
9	100	1.54	-1.86	0.74	0.8787
10	100	1.82	-1.82	0.68	0.8353

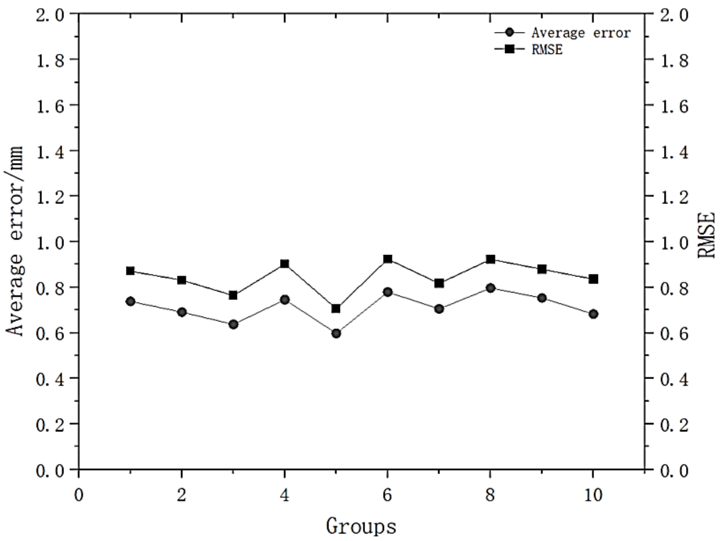

Fig. 16 – Error of control system and algorithm

The maximum measurement error, the minimum measurement error, the average measurement error and root mean square error were shown in Table 3, and the error generated by the control system and the cam inversion algorithm was generally larger than the error in the last experiment.

From the trend of the curves in Fig. 16, the average errors were relatively stable in the range of 0.6-0.8 mm. Under the same experimental conditions, the root mean square errors of the ten groups were maintained at a low level, and the accuracy of motion control and calculation in the cam inversion algorithm was stable.

Girdling operation error

In this experiment, a wooden pile with its complete bark structure was selected to be girdled. In order to ensure the accuracy of the scanning profile, the number of measurement points was 600 in the process of scanning. In this experiment, the device took 30 seconds to scan the wooden pile, and it took 120 seconds for the chainsaws to perform girdling. The difference between the surface after girdling and the xylem of the wooden pile was defined as the girdling overall error, and the errors were measured by 50 index vernier scale. The processes of scanning and girdling were shown in Fig.17 and Fig.18. In Fig.19, the red curve was the scanning profile of the wooden pile, and the brown curve was the girdling profile at the corresponding cross-section of the wooden pile. The xylem profile was obtained by the interval minimum algorithm mentioned in Fig. 7.

Fig. 17 – Scanning

Fig. 18 – Girdling

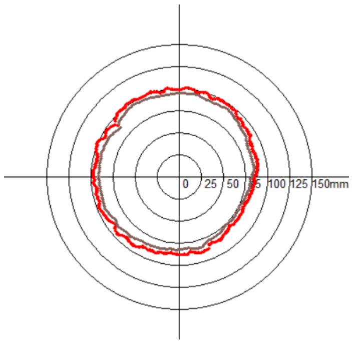

Fig. 19 – Scanning profile and xylem profile

Table 4

Error of the girdling device

Experimental group	Number of measurement points	Maximum error (mm)	Minimum error(mm)	Average error(mm)	Root mean square error
1	100	1.98	-1.98	1.04	1.1882
2	100	1.94	-1.92	0.96	1.1145
3	100	1.96	-1.92	1.12	1.1742
4	100	1.98	-1.95	0.84	1.0198
5	100	1.96	-1.98	0.99	1.1649
6	100	1.96	-1.96	0.96	1.1344
7	100	1.96	-1.94	0.98	1.1401
8	100	1.96	-1.92	0.94	1.1246
9	100	1.98	-1.96	1.06	1.2205
10	100	1.94	-1.94	1.02	1.1578

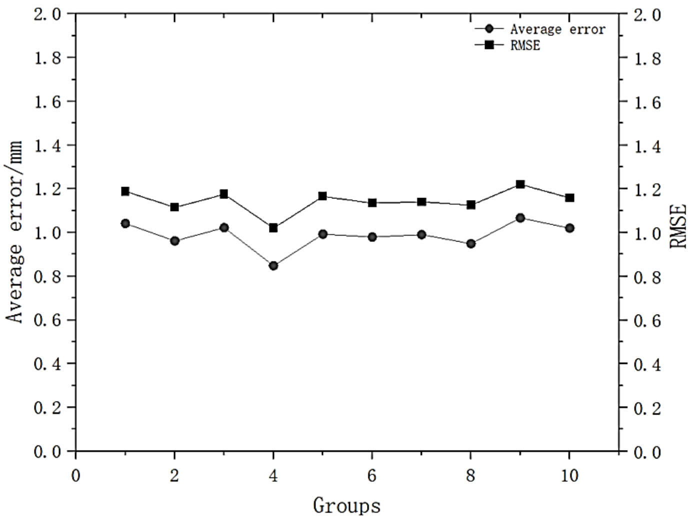

Fig. 20 –Error of the girdling device

The error generated by girdling was accumulated by the profile scanning error, motion control error and calculation error from algorithm. The new error in this experiment was from the calculation error in interval minimum algorithm. Because only one point was selected from the interval, there were differences between the calculated xylem profile by the interval minimum algorithm and the real xylem profile. The error was accumulated, and it effected the calculation in the cam inversion algorithm. The maximum error, minimum error, average error and root mean square error were shown in Table 4. The trends of average error and root mean square error were shown in Fig. 20. The comprehensive error of girdling was within ±2 mm, and the average error was within 1.1 mm, and the girdling error of this device was relatively stable.

CONCLUSIONS

(1) The mechanical structure for the automatic girdling device was verified. In the rotation process of the half-ring rail, the scanning of the tree trunk profile was realized by two symmetrical laser rangefinders at the end of the half-ring rail. In the combined motion of the half-ring rail rotational motion and the guide screws radial motion, the girdling of the tree trunk was realized by two chainsaws above the guide screws.

(2) The control program for the girdling operation was implemented in LabVIEW, and the feasibility of the control program was proved within the girdling experiments. The minimum interval algorithm was presented to acquire the xylem profile according to tree trunk profile. The cam inversion algorithm was proposed to obtain the chainsaw centre trajectory according to the xylem profile.

(3) The error analysis experiments of the device were divided into three steps. The error analysis of the device scanning system was carried out by comparing with the measurement result from the RA7525SE-1005. The motion control error and algorithm calculation error were obtained by cutting the wooden pile only with the xylem. The girdling operation error was tested by girdling the complete trunk. The girdling error is within ±2 mm and the overall time of girdling is within 150 seconds, and the accuracy and efficiency for economic tree trunk girdling can be improved with this device.

ACKNOWLEDGEMENT

This work is supported by the Fundamental Research Funds for the Central Universities (2017ZY46) and 2023HXKFGXY002.

REFERENCES

[1] Chai, L., Li, Q., Wang, H., Wang, C., Xu, H., Jiang, W., (2021). Girdling alters carbohydrate allocation to increase fruit size and advance harvest in tomato production, *Scientia Horticulturae*, Vol.276, Amsterdam/ Netherlands.

[2] De Schepper, V., Steppe, K., (2011). Tree girdling responses simulated by a water and carbon transport model. *Annals of Botany*, Vol.108, Issue 6, pp.1147–1154, Oxford/England.

[3] Duan, L., (2007). Review of girdling knife development and innovative tool outlook (环剥刀研制的回顾与创新刀具展望), *Shanxi Fruits*, Vol.1, pp.37–38, 39, Shanxi/China.

[4] Goren, R., Huberman, M., Goldschmidt, E.E., 2004. Girdling: physiological and horticultural aspects. *Hortic. Rev*. 30, 1–36. https://doi.org/10.1002/9780470650837.ch1.

[5] Gülden G., Atalba M.C., Guler H., (2020), Chaotic Systems Based Real-Time Implementation of Visual Cryptography Using LabVIEW. *Traitement du Signal*, Vol 37, Issue 4, pp. 639 -645, Turkey;

[6] Juan, M., Mesejo, C., Martínez-Fuentes, A., Reig, et al., (2009), Branch scoring encourages fruit development and climacteric in persimmon. *Scientia Horticulturae*, Vol.122, Issue 3, pp.497–500, Amsterdam / Netherlands.

[7] Li, H., Xie, J., (2019). Research Status and Countermeasures of Jujube Girdling Technology (枣树环剥技术研究现状与对策), *Journal of Tarim University*, Vol.31, Issue 1, pp.89–93, Xinjiang/China.

[8] Michailidis M., Karagiannis E., Tanou G., et al., (2020). Proteomic and metabolic analysis reveals novel sweet cherry fruit development regulatory points influenced by girdling. *Plant Physiol Biochem*, Vol.149, pp.233–244. Issy-les-Moulineaux / France.

[9] Oberhunber, W., Gruber, A., Lethaus, G., Winkler, A., Wieser, G. (2017). Stem girdling indicates prioritized carbon allocation to the root system at the expense of radial stem growth in Norway spruce under drought conditions, *Environmental and Experimental Botany*, Vol.138, pp.109–118, Austria.

[10] Olofsson, K., Holmgren, J., (2016). Single Tree Stem Profile Detection Using Terrestrial Laser Scanner Data, Flatness Saliency Features and Curvature Properties, *Forests*, Vol.7, Issue.9, pp.1-23, Basel / Switzerland.

[11] Wilkie, J.D., Sedgley, M., Olesen, T., (2008), Regulation of floral initiation in horticultural trees. *Journal of Experimental Botany*, Vol. 59, Issue 12, pp. 3215–3228, NSW / Australia. https://doi.org/10.1093/jxb/ern188.
[12] Xie, J., Li, H., Jiang, X., et al., (2018). Research and Design of Electric Type Jujube Tree Ring Cutting Machine (电动式枣树环剥机的设计研究), *Science & Technology Vision*. pp.64–65, Xinjiang/China.
[13] Yang, X., Wang, F., Jaime, A.T.D.S., Zhong, J., et al., (2013), Branch girdling at fruit green mature stage affects fruit ascorbic acid contents and expression of genes involved in l-galactose pathway in citrus. New Zealand Journal of Crop and Horticultural Science, Vol.41, Issue 1, pp.23–31, Beijing / China.
[14] Ye, B., Xie, S., Zhang, J., et al., (2019). Effect of Ring Peeling on Jujube Growth and Fruit Quality (枣树环剥对枣树生长及果实品质的影响), *Agricultural technology and equipment*, pp.30–32, Gansu/China.
[15] Zhang X., Hou Z., Dai N., (2021), Design and experiment of a new rotary coating machine based on LabVIEW. *INMATEH Agricultural Engineering*, Vol 65, Issue 3, pp. 91-100, China. https://doi.org/10.35633/inmateh-65-10
[16] Zhu, M., Yu, J., Xu, Yang, G., (2022). Effect of Girdling on Anthocyanin Content and Quality of Spine Grape Berries. *Journal of Plant Growth Regulation*, Vol.41, Issue 1, pp.65–73, New York/American.